Journal of Sound and Vibration (1997) **199**(1), 51–69

STABILITY AND VIBRATION OF INITIALLY STRESSED PLATES COMPOSED OF SPATIALLY DISTRIBUTED FIBER COMPOSITES

W. S. KUO† AND J. H. HUANG‡

Department of Textile Engineering† and Department of Mechanical Engineering‡, Feng Chia University, Taichung, Taiwan, Republic of China

(*Received* 20 *October* 1995; *and in final form* 21 *May* 1996)

Three groups of elastic constants, defined as *orthotropic constants*, have been introduced in this paper, and utilizing these constants enables the transformed stiffness to be expressed in rather simple forms. To simulate spatial fiber orientation in a preferred direction, a distribution function controlled by two parameters is introduced. The equivalent composite elastic properties are then simulated by an aggregated model. Three special cases for fiber orientation have been discussed and the closed-form stiffnesses have bene obtained. Equations of motion for a composite plate in a general state of non-uniform initial stresses, where the effects of transverse shear and rotatory inertia are included, are derived by using Trefftz equations and the variational principle. Finally, the stability and vibration equations are solved for simply supported rectangular plates in a state of normal stresses plus an edge twisting stress. The effect of fiber orientation on the fundamental frequencies and buckling loads has been discussed.

1. INTRODUCTION

Fiber architecture has been considered to be the most important feature in composite design. Placing fibers where they are needed is a direct and efficient method of using the fibers to improve composite performance. Depending on the loading conditions and structural requirements, the orientation of the fibers in a composite can be linear, planar, or spatial. In recent years, composites composed of spatially distributed fibers have become popular in a wide variety of applications, especially through fabrication techniques such as injection molding, bulk molding compound, and three-dimensional weaving and braiding. Using spatial fibers as reinforcing elements in a controlled manner could provide more balanced properties, which leads to an improved through-the-thickness stiffness/strength and a better ability to formulate complex shapes. However, it is almost impossible to control the movement of fibers in perfect alignment. A probabilistic study on fiber orientation is therefore necessary. Instead of the unachievable perfect alignment, partial alignment is typical, indicating that fibers are oriented in a preferred direction. In principle, the distribution of fiber orientation can be represented by either a density function or a cumulative function, although the function is quite hard to obtain without the help of computers together with the techniques such as laser beam scatter optical scanner and image analysis [1–3].

As spatially reinforced composites gain popularity, the need for a basic understanding of the composites grows. The most essential material properties of such a composite are elastic constants, which govern the composite static and dynamic behavior. Several approaches have been proposed in predicting their effective properties. Micromechanics

0022–460X/97/010051 + 19 $25.00/0/sv960629

focusing on the interactions between inhomogeneities (or inclusions) and the surrounding matrix can be the most powerful tools [4–6], although mathematical formulations can be very complex, and limitation still exists when applied to rather high fiber volume fractions. Another method is the so-called aggregate model [7, 8], used mainly for cases with irregular fiber orientation. Although the latter approach might be unable to reflect the geometrical aspects of composites, it provides for a simple means to examine the effect of the component distribution on the overall properties, and this method is even more suitable for handling higher fiber fraction. Therefore, the concept of the aggregate model will be used in this paper.

It is known that initial stresses can be due to several sources, such as thermal expansion mismatch, plastic deformation, or residual stress during the curing of composites. These initial stresses could significantly affect its structural behavior. For better material utilization, a controlled prestressing for advanced fiber-reinforced composite structures is feasible. Therefore, the prediction of the stability and dynamic behavior of a plate under initial stress has attracted considerable attention [9–11]. Undoubtedly, a study of thick plates in an arbitrary state of initial stress will provide structural engineers with more information about plate behavior.

The purpose of this paper is to investigate the effect of initial stresses on the buckling and vibration response of thick plates. The framework for this study is based on Trefftz's definition of stress [12, 13] and Mindlin plate theory in which both rotatory inertia and shear deformation effects are taken into account. No terms are dropped unnecessarily, and the equation derived here can be used to study non-linear post-buckling and large deformation vibration behavior as well as non-conservative stability and dynamic problems for various states of initial stresses. In the work described herein, the equations for initially stressed thick plates have been applied to simply supported rectangular plates subjected to in-plane normal stresses and a twisting stress acting on the edges of the plate.

2. THREE-DIMENSIONAL TRANSFORMATIONS

In the first part of the present work, an attempt is made to accomplish the 3-D elastic transformation that is essential concerning a rotated element. The (1, 2, 3) system is termed the material co-ordinate since this co-ordinate is defined to relate the local principal material directions; and (x, y, z) system is termed the geometrical coordinate for referring to the global structure geometry. For an orthotropic element arbitrarily placed in space, its orientation can be expanded by three linearly independent rotational vectors.

To represent the 3-D orientation, the following three-step rotation is adopted as shown in Figure 1. First, the rotation of an angle θ about the z-axis of the original co-ordinate (x, y, z) yields a co-ordinate (x', y', z'). Then, the rotation of an angle ϕ with respect to the y'-axis results in the (x'', y'', z'') co-ordinate. Finally, the rotation of an angle ω with respect to the z''-axis generates the (x''', y''', z''') co-ordinate. The (1, 2, 3) system is then designed to be coincident with the (x''', y''', z''') system. Note that the θ, ϕ, and ω are usually termed as *Euler* angles. The geometrical relations of θ, ϕ, and ω in a spatial rotation are illustrated in Figure 2.

Giving a set of (θ, ϕ, ω) should uniquely determine an orientation and *vice versa* except $\phi = 0$ or π, in which cases θ and ω are linearly dependent. It should be noted that the order of the rotations is *not* commutative; different rotational ordering of an identical set of angles can result in dissimilar orientations.

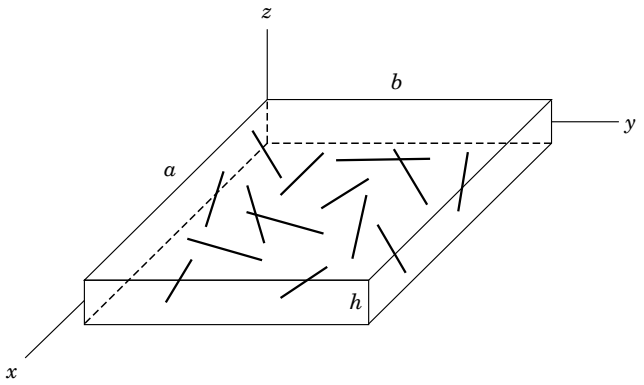

Figure 1. Schematic drawing of spatially orientated fibers in a plate.

Let u_1, u_2 and u_3 be the unit vectors in the (1, 2, 3) coordinate and u_x, u_y and u_z be the unit vectors in the (x, y, z) coordinate. The relations between these two sets of vectors can be expressed as

$$\begin{bmatrix} u_x \\ u_y \\ u_z \end{bmatrix} = \begin{bmatrix} mpr - ns & -mps - nr & mq \\ npr + ms & mr - nps & nq \\ -qr & qs & p \end{bmatrix} \begin{bmatrix} u_1 \\ u_2 \\ u_3 \end{bmatrix}, \tag{1}$$

where the symbols are $m = \cos(\theta)$, $n = \sin(\theta)$, $p = \cos(\phi)$, $q = \sin(\phi)$, $r = \cos(\omega)$, and $s = \sin(\omega)$.

Since both stress and strain are second-order tensors, the transformation between these two co-ordinates can be readily obtained using tensor transformation laws. The engineering shear strains are two times the corresponding tensorial shear strains. Thus, to

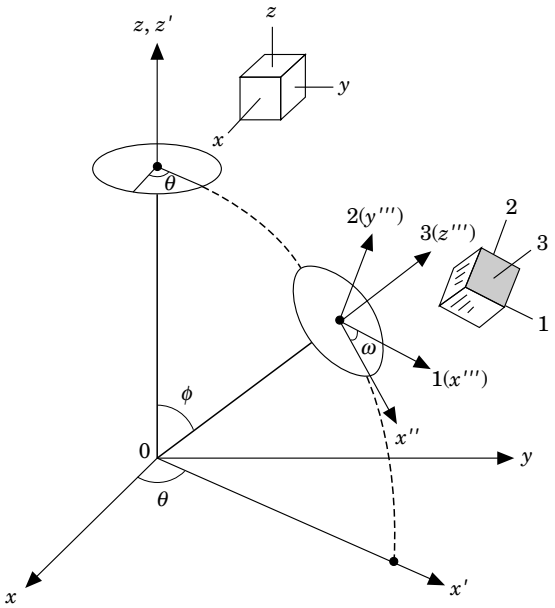

Figure 2. Three-dimensional rotation of a spatially oriented element.

relate these two sets of strains, a 6×6 diagonal matrix $[R]$, in which the diagonal terms are $\{1, 1, 1, 2, 2, 2\}$, is introduced. Denote the stiffness with respect to (1, 2, 3) and (x, y, z) systems as [Q] and $[\bar{Q}]$ respectively. For an orthotropic material with nine constants, the non-zero terms in [Q] are Q_{11}, Q_{12}, Q_{13}, Q_{22}, Q_{23}, Q_{33}, Q_{44}, Q_{55}, and Q_{66}. Using tensor laws, the transformed stiffness matrix can be easily proven to be

$$[\bar{Q}] = [T]^{-1}[Q][R][T][R]^{-1}, \tag{2}$$

where [T] is the stress transformation matrix, which can be established from the co-ordinate transformation matrix in equation (1) using the second-order tensor law. The details of [T] are listed in the Appendix, Equation (A1). All matrices in equation (2) are 6×6.

Equation (2) can be easily evaluated based on numerical computations providing that all Q_{ij} and the angles are given numerically. However, direct mathematical solutions not only provide an easier way to obtain numerical values, but more importantly offer a comprehensive tool that could elucidate the fundamental nature of transformed properties. Nevertheless, direct symbolic expansions of equations (2), involving multiplication of five 6×6 matrices, contain too many terms to have hardly any practical applicability from an engineering design point of view. In dealing with this difficulty, three special material constants have been found to be helpful. These material constants are termed as *orthotropic constants* for orthotropic materials as following.

$$K_1 = Q_{22} + Q_{33} - 2Q_{23} - 4Q_{44}, \qquad K_2 = Q_{33} + Q_{11} - 2Q_{13} - 4Q_{55},$$
$$K_3 = Q_{11} + Q_{22} - 2Q_{12} - 4Q_{66}. \tag{3}$$

It is clear that the K's are cyclic with respect to axes 1, 2, and 3. Physically, they might be interpreted as *deviations* from an isotropic medium since $K_1 = K_2 = K_3 = 0$ for an isotropic medium.

By incorporating these orthotropic constants, the terms in each $\bar{Q}_{ij}$ are greatly simplified and can be expressed in a minimum number of terms as listed in the Appendix, equation (A2). The transformation for the compliance matrix can be similarly treated and is not listed herein.

3. COMPOSITE COMPOSED OF RANDOMLY ORIENTED FIBERS

In this section, effective elastic properties of a composite containing randomly oriented orthotropic fibers are discussed. It is assumed that the composite contains multiple material components. Each component can have distinct material properties. For the composite studied, the components are fibers and matrix. The rotational angles of a fiber can generally be represented by the three angles ϕ, θ, and ω. The concept of *aggregate modeling* has been used for evaluating effective moduli of composites. Averaged composite stiffnesses can be calculated according to

$$\hat{Q}_{ij} = \frac{1}{V}\int_V \bar{Q}_{ij}(v)\,\mathrm{d}v$$

$$= V_f \int_0^{2\pi}\int_0^{\pi}\int_0^{2\pi} \bar{Q}^f_{ij}(\theta, \phi, \omega)\beta(\theta, \phi, \omega)\sin(\phi)\,\mathrm{d}\omega\,\mathrm{d}\phi\,\mathrm{d}\theta + (1 - V_f)Q^m_{ij}, \tag{4}$$

where V_f is the total fiber volume fraction in the composite, $\bar{Q}^f_{ij}$ the stiffness of a fiber, Q^m_{ij} the stiffness of the matrix, and $\beta(\theta, \phi, \omega)$ the probability density function for the

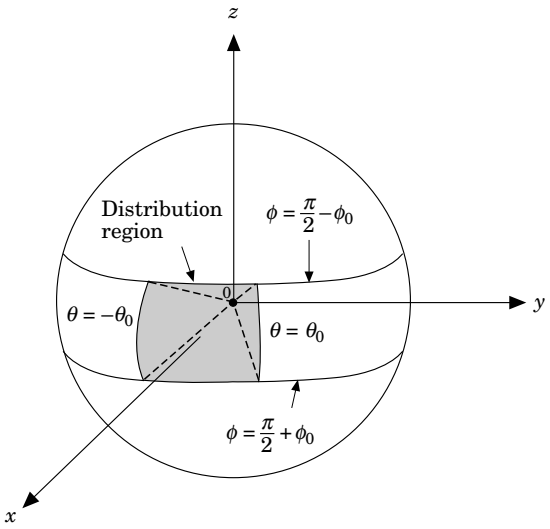

Figure 3. Fiber distribution in a preferred direction.

distribution of fiber orientation. Sin (ϕ) in the integrand of equation (4) is to account for the surface area of a sphere. In consideration of composite processing, fiber orientation distribution might depend on position, resulting in a macroscopically inhomogeneous composite. To simplify the analysis, only when β is independent of position is discussed. Since the matrix is isotropic and is independent of rotation, equation (4) can be simplified by introducing Q_{ij} and $\bar{Q}_{ij}$ defined as

$$Q_{ij} = V_f Q_{ij}^f + (1 - V_f) Q_{ij}^m, \qquad \bar{Q}_{ij} = V_f \bar{Q}_{ij}^f + (1 - V_f) Q_{ij}^m \tag{5}$$

As a result of the aggregate model, equation (5) is known to be most suitable for predicting elastic constants that are dominated by fibers. For example, for a unidirectional composite equation (5) can predict the longitudinal modulus better than the transverse and shear moduli, which are matrix controlled. Therefore, for a composite possessing well-distributed fibers and no specific direction in which the fiber content is extremely low, such as the one discussed in this paper, equation (5) would be adequate. Modified forms of equation (5) based upon micromechanics or empirical data for certain types of composites can be found in the literature [14–16]. Incorporating equation (5) with equation (4) results in

$$\hat{Q}_{ij} = \int_0^{2\pi} \int_0^{\pi} \int_0^{2\pi} \bar{Q}_{ij}(\theta, \phi, \omega) \beta(\theta, \phi, \omega) \sin(\phi)\, \mathrm{d}\omega\, \mathrm{d}\phi\, \mathrm{d}\theta \tag{6}$$

Once the $\beta(\theta, \phi, \omega)$ is given, $\hat{Q}_{ij}$ can be evaluated symbolically or numerically. To illustrate how fiber orientation affects the composite elastic and mechanical behavior, discussed herein is the case in which fibers are spatially distributed in a preferred direction. Let the preferred direction be the x-axis. As shown in Figure 3, fibers are assumed to be uniformly distributed over the given region; namely, β is a constant over the region. The corresponding distribution region is defined by

$$-\theta_0 \leqslant \theta \leqslant \theta_0,\ \pi/2 - \phi_0 \leqslant \phi \leqslant \pi/2 + \phi_0,\ 0 \leqslant \omega \leqslant 2\pi \tag{7}$$

where θ_0 and ϕ_0 are prescribed values, and ω is so given that any fiber is free to rotate with respect to its axial direction. From equation (7), the corresponding density function is found to be

$$\beta(\theta, \phi, \omega) = 1/8\pi\theta_0 \sin(\phi_0) \tag{8}$$

Thus, equation (6) becomes

$$\hat{Q}_{ij} = \frac{1}{8\pi\theta_0 \sin(\phi_0)} \int_{-\theta_0}^{\theta_0} \int_{\pi/2-\phi_0}^{\pi/2+\phi_0} \int_0^{2\pi} \bar{Q}_{ij}(\theta, \phi, \omega) \sin(\phi)\, d\omega\, d\phi\, d\theta \tag{9}$$

The explicit result of the integration in equation (9) can be obtained for any given θ_0 and ϕ_0 since the solutions of $\bar{Q}_{ij}$ have been obtained explicitly. However, the general explicit results for $\hat{Q}_{ij}$ could be quite lengthy, and listed here are only the following special cases.

(a) $\theta_0 \to 0$, $\phi_0 \to 0$. This represents the situation in which all fibers are aligned and parallel to the x-axis, and hence fibers are free to rotate only with respect to the three axial directions. By substituting equation (A-2) into equation (9) and performing the integration, one finds that the non-zero $\hat{Q}_{ij}$ terms are

$$\hat{Q}_{11} = Q_{33}, \qquad \hat{Q}_{22} = \hat{Q}_{33} = \tfrac{1}{2}(Q_{11} + Q_{22}) - \tfrac{1}{8}K_3, \qquad \hat{Q}_{23} = Q_{12} + \tfrac{1}{8}K_3,$$
$$\hat{Q}_{12} = \hat{Q}_{13} = \tfrac{1}{2}(Q_{13} + Q_{23}), \qquad \hat{Q}_{44} = Q_{66} + \tfrac{1}{8}K_3, \qquad \hat{Q}_{55} = \hat{Q}_{66} = \tfrac{1}{2}(Q_{44} + Q_{55}) \tag{10}$$

It can be proved that $\hat{Q}_{44} = (\hat{Q}_{22} - \hat{Q}_{23})/2$, indicating that yz-plane is the plane of isotropy and the composite is transversely isotropic. The resulting composite includes five elastic constants.

(b) $\theta_0 = \pi$, $\phi_0 \to 0$. This represents the case in which fibers are uniformly lying on the xy-plane, and is therefore a two-dimensional in-plane distribution. The non-zero terms are

$$\hat{Q}_{11} = \hat{Q}_{22} = \tfrac{1}{4}(Q_{11} + Q_{22}) + \tfrac{1}{2}Q_{33} - \tfrac{1}{16}(K_1 + K_2) - \tfrac{3}{64}K_3, \qquad \hat{Q}_{33} = \tfrac{1}{2}(Q_{11} + Q_{22}) - \tfrac{1}{8}K_3,$$
$$\hat{Q}_{23} = \hat{Q}_{13} = \tfrac{1}{4}(Q_{13} + Q_{23}) + \tfrac{1}{2}Q_{12} + \tfrac{1}{16}K_3, \qquad \hat{Q}_{12} = \tfrac{1}{2}(Q_{13} + Q_{23}) + \tfrac{1}{16}(K_1 + K_2) - \tfrac{1}{64}K_3,$$
$$\hat{Q}_{44} = \hat{Q}_{55} = \tfrac{1}{4}(Q_{44} + Q_{55}) + \tfrac{1}{2}Q_{66} + \tfrac{1}{16}K_3, \qquad \hat{Q}_{66} = \tfrac{1}{2}(Q_{44} + Q_{55}) + \tfrac{1}{16}(K_1 + K_2) - \tfrac{1}{64}K_3. \tag{11}$$

It can be proved that $\hat{Q}_{66} = (\hat{Q}_{11} - \hat{Q}_{12})/2$, indicating that the xy-plane is the plane of isotropy, and the composite is transversely isotropic with respect to the z-axis, and among the nine non-zero terms, five are independent.

(c) $\theta_0 = \pi$, $\phi_0 \to \pi/2$. This represents the case in which fibers are uniformly distributed in all directions, which may be termed as *completely random distribution*. From the definition, the composite behavior should be independent of direction, or the composite is isotropic. The non-zero terms are

$$\hat{Q}_{11} = \hat{Q}_{22} = \hat{Q}_{33} = \tfrac{1}{3}(Q_{11} + Q_{22} + Q_{33}) - \tfrac{1}{15}(K_1 + K_2 + K_3),$$
$$\hat{Q}_{12} = \hat{Q}_{13} = \hat{Q}_{23} = \tfrac{1}{3}(Q_{23} + Q_{13} + Q_{12}) + \tfrac{1}{30}(K_1 + K_2 + K_3),$$
$$\hat{Q}_{44} = \hat{Q}_{55} = \hat{Q}_{66} = \tfrac{1}{3}(Q_{44} + Q_{55} + Q_{66}) + \tfrac{1}{30}(K_1 + K_2 + K_3). \tag{12}$$

Due to symmetric distribution of yarn orientation, the composite as a whole is macroscopically isotropic; this can be easily proved from the fact that $\hat{Q}_{44} = (\hat{Q}_{11} - \hat{Q}_{12})/2$. According to the theory of elasticity, Young's modulus E and Poisson ratio v can be obtained as

$$E = [(\hat{Q}_{11} - \hat{Q}_{12})(\hat{Q}_{11} + 2\hat{Q}_{12})/(\hat{Q}_{11} + \hat{Q}_{12}), \qquad v = \hat{Q}_{12}/(\hat{Q}_{11} + \hat{Q}_{12}) \tag{13}$$

The above constants can be in turn expressed by the basic engineering constants of the fiber and matrix.

Once the stiffness matrix $[\hat{Q}]$ is obtained from equation (9), the inversion of the stiffness matrix results in the compliance matrix $[\hat{S}]$ from which the composite engineering constants including Young's moduli (E_x, E_y, E_z), shear moduli (G_{yz}, G_{xz}, G_{xy}), and Poisson ratio (v_{yz}, v_{xz}, v_{xy}) can be calculated. Note that the Young's and shear moduli predicted by this stiffness approach is a known upper-bound solution; on the other hand, a compliance approach yields a lower-bound solution. Both bounds can be obtained by the methodology developed in this paper, and the characteristics of the bounds depend on the K's; detailed discussion on this topic is not presented herein.

4. VARIATIONAL FORMULATION FOR PLATE GOVERNING EQUATIONS

This section examines the governing equation of motion for a plate composed of spatially reinforced fiber composite and subjected to initial stresses. According to Bolotin [13] the equilibrium equation and boundary traction condition in tensor forms can be expressed in terms of Trefftz stress components as

$$\begin{aligned}[t_{ij}(u_s + u_s^0)_{,j} + \sigma_{ij}(\delta_{sj} + u_{s,j} + u_{s,j}^0)]_{,i} + X_s^0 + X_s + \Delta X_s - \rho\ddot{u}_s = 0,\\ P_s^0 + p_s + \Delta P_s = [t_{ij}(u_s + u_s^0)_{,j} + \sigma_{ij}(\delta_{sj} + u_{s,j} + u_{s,j}^0)]n_i,\end{aligned} \tag{14}$$

where t_{ij}, u_s^0, X_s^0 and P_s^0 stand for the initial stress, displacement, body force, and surface traction respectively, and σ_{ij}, u_s, X_s and p_s are the corresponding perturbation quantities. The terms ΔX_s and ΔP_s represent changes in the body force and surface traction due to perturbation.

Since the composite is in an equilibrium state before perturbation, the equation for incremental stresses and displacements can be reduced as follows:

$$\begin{aligned}(t_{ij}u_s)_{,i} + [\sigma_{ij}(\delta_{sj} + u_{s,j} + u_{s,j}^0)]_{,i} + X_s + \Delta X_s - \rho\ddot{u}_s = 0,\\ p_s + \Delta P_s = [t_{ij}u_{s,j} + \sigma_{ij}(\delta_{sj} + u_{s,j} + u_{s,j}^0)]n_i.\end{aligned} \tag{15}$$

The equation of the virtual work can be obtained by multiplying equation (15) by the variation of the displacement component δu_s and then integrating the resulting expression over the initial volume V. Upon using the product differentiation rules and the divergence theorem, the equation becomes

$$\delta(\bar{V} + \bar{W}) + \int_V \rho\ddot{u}_s\delta u_s \, \mathrm{d}v = \int_s [t_{ij}u_{s,j} + \sigma_{is} + \sigma_{ij}(u_{s,j} + u_{s,j}^0)]\delta u_s n_i \, \mathrm{d}s + \int_v (X_s + \Delta X_s)\, \delta u_s \, \mathrm{d}v, \tag{16}$$

where

$$\delta\bar{V} = \delta \int_v \tfrac{1}{2}\sigma_{ij}\varepsilon_{ij} \, \mathrm{d}v, \qquad \delta\bar{W} = \delta \int_v \tfrac{1}{2}t_{ij}u_{s,i}u_{s,j} \, \mathrm{d}v \tag{17}$$

The surface integral in equation (16) consists of the integration over the areas S_p and S_u in which surface tractions and displacements are prescribed respectively. Therefore, from the second of equation (15), the virtual work theorem is finally represented as

$$\begin{aligned}\delta(\bar{V} + \bar{W}) + \int_V \rho\ddot{u}_s\delta u_s \, \mathrm{d}v = &\int_{S_p} (p_s + \Delta P_s)\delta u_s \, \mathrm{d}s\\ &+ \int_{S_u} [t_{ij}u_{s,j} + \sigma_{is} + \sigma_{ij}(u_{s,j} + u_{s,j}^0)]\delta u_s n_i \, \mathrm{d}s\\ &+ \int_v (X_s + \Delta X_s)\, \delta u_s \, \mathrm{d}v.\end{aligned} \tag{18}$$

The tensor form of the virtual work theorem is valid not only for linear and conservative problems but also non-linear and non-conservative ones. The equation will be used subsequently in deriving the equations of motion for arbitrarily prestressed plates.

In dealing with the perturbing displacements in a plate, several displacement functions have been used. For rather thin plates, Kirchhoff types of displacement functions could be sufficient. For thick plates and detailed three-dimensional displacement and stress analysis within a plate, many higher order functions with rather complex analysis have been proposed [17, 18]. Taking into account both displacement and stress continuities within an elastic body and on boundary surfaces these theories generally yield better results and inevitably require elaborated equation manipulations and numerical computations. For the sake of simplicity, Mindlin plate theory [9–11] is adopted in this paper:

$$u_1(x, y, z, t) = u(x, y, t) + z\Psi_x(x, y, t), \qquad u_2(x, y, z, t) = v(x, y, t) + z\Psi_y(x, y, t),$$

$$u_3(x, y, z, t) = w(x, y, t). \tag{19}$$

where u, v, and w are mid-plane displacements in x-, y-, and z-directions respectively, and Ψx and Ψ_y are rotatory angles.

For a linear elastic plate, the constitutive equation is

$$\begin{bmatrix} \sigma_{xx} \\ \sigma_{yy} \\ \sigma_{yz} \\ \sigma_{xz} \\ \sigma_{xy} \end{bmatrix} = \begin{bmatrix} \hat{Q}_{11} & \hat{Q}_{12} & \hat{Q}_{14} & \hat{Q}_{15} & \hat{Q}_{16} \\ \hat{Q}_{12} & \hat{Q}_{22} & \hat{Q}_{24} & \hat{Q}_{25} & \hat{Q}_{26} \\ \hat{Q}_{14} & \hat{Q}_{24} & \hat{Q}_{44} & \hat{Q}_{45} & \hat{Q}_{46} \\ \hat{Q}_{15} & \hat{Q}_{25} & \hat{Q}_{45} & \hat{Q}_{55} & \hat{Q}_{56} \\ \hat{Q}_{16} & \hat{Q}_{26} & \hat{Q}_{46} & \hat{Q}_{56} & \hat{Q}_{66} \end{bmatrix} ([\varepsilon_0] + z[\kappa]), \tag{20}$$

where

$$[\varepsilon_0] = [u_{,1}, v_{,2}, w_{,2} + \Psi_y, w_{,1} + \Psi_x, u_{,2} + v_{,2}]^T, \qquad [\kappa] = [\Psi_{x,1}, \Psi_{y,2}, 0, 0, \Psi_{x,2} + \Psi_{y,1}]^T \tag{21}$$

and $\hat{Q}_{ij}$ are transformed reduced stiffnesses for the composite as defined in equation (9).

The force and moment resultants in the plate are defined as

$$[N_x, N_y, Q_y, Q_x, N_{xy}] = \int_{-h/2}^{h/2} [\sigma_{xx}, \sigma_{yy}, \sigma_{yz}, \sigma_{xz}, \sigma_{xy}]^T \, \mathrm{d}z,$$

$$[M_x, M_y, M_{yz}, M_{xz}, M_{xy}] = \int_{-h/2}^{h/2} z[\sigma_{xx}, \sigma_{yy}, \sigma_{yz}, \sigma_{xz}, \sigma_{xy}]^T \, \mathrm{d}z. \tag{22}$$

The plate extensional, coupling, and bending stiffnesses are defined as

$$(A_{ij}, B_{ij}, D_{ij}) = \int_{-h/2}^{h/2} \hat{Q}_{ij}(1, z, z^2) \, \mathrm{d}z \tag{23}$$

Consider a plate with side length a and b and thickness h as shown in Figure 1. Also, assume that the system is conservative and that no transverse initial stresses act on the plate. Performing all the integrations in equation (18), taking variations with respect to

all variables, neglecting small terms and collecting terms that contain variations of the same displacements, one obtains

$$\int_0^a \int_0^b \{H_1\delta_u + H_2\delta_v + H_3\delta w + H_4\delta\Psi_x + H_5\delta\Psi_y\}\,\mathrm{d}y\,\mathrm{d}x$$

$$+ \int_0^a [I_1\delta_u + I_2\delta_v + I_3\delta w + I_4\delta\Psi_x + I_5\delta\Psi_y]_{y=0}^{y=b}\,\mathrm{d}x$$

$$+ \int_0^b [J_1\delta_u + J_2\delta_v + J_3\delta w + J_4\delta\Psi_x + J_5\delta\Psi_y]_{x=0}^{x=a}\,\mathrm{d}y = 0, \tag{24}$$

where H_i, I_i, J_i consist of the displacement functions (equation (19)), the stiffnesses (equation (23)), and the initial forces and moments. The details of H_i, I_i, and J_i are listed in the Appendix, equation (A3). The initial forces and moments in E_i, F_i, and G_i, denoted as barred N's and M's, are defined as

$$(\bar{N}_x, \bar{N}_y, \bar{N}_{xy}) = \int_{-h/2}^{h/2} (t_{11}, t_{22}, t_{12})\,\mathrm{d}z, \qquad (\bar{M}_x, \bar{M}_y, \bar{M}_{xy}) = \int_{-h/2}^{h/2} (t_{11}, t_{22}, t_{12})z\,\mathrm{d}z,$$

$$(\bar{M}_x^*, \bar{M}_y^*, \bar{M}_{xy}^*) = \int_{-h/2}^{h/2} (t_{11}, t_{22}, t_{12})z^2\,\mathrm{d}z. \tag{25}$$

The initial normal stresses are assumed to be constants and the shear stress linear as shown in Figure 4:

$$t_{11} = \sigma_{x_0}, \qquad t_{22} = \sigma_{y_0}, \qquad t_{12} = (2z/h)\tau_0 \tag{26}$$

and all other initial stresses vanish. The stresses σ_{x_0}, σ_{y_0}, and τ_0 are constants so that the initial stresses are uniform. The non-zero initial forces and moments are

$$(\bar{N}_x, \bar{N}_y) = (\sigma_{x_0}, \sigma_{y_0})h, \qquad \bar{M}_{xy} = \tau_0 h^2/6,$$

$$(\bar{M}_x^*, \bar{M}_y^*) = (\sigma_{x_0}, \sigma_{y_0})h^3/12. \tag{27}$$

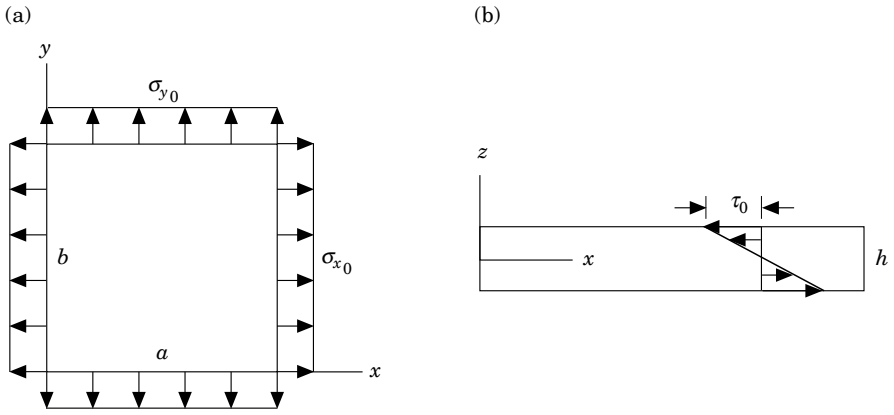

Figure 4. An initially stressed plate: (a) normal stresses; (b) shear stress.

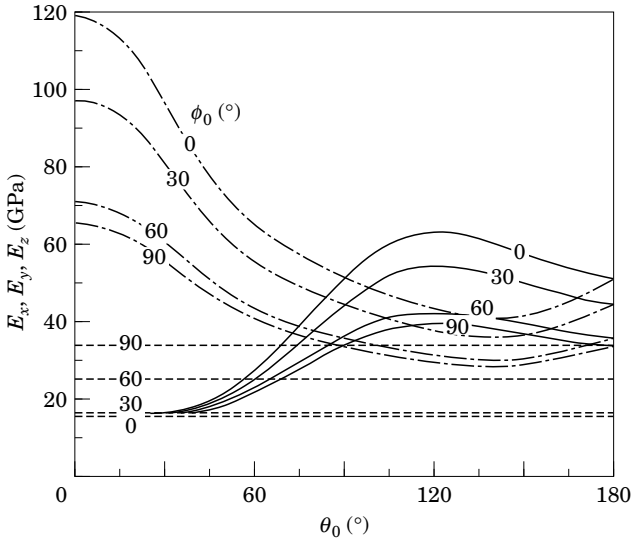

Figure 5. Young's moduli versus θ_0 for various ϕ_0: —·—, E_x; ——, E_y; – – –, E_z.

For simply supported plates, the following displacement functions satisfying the boundary conditions are introduced:

$$u = C_1 h \sin(\xi)\cos(\eta)\, e^{i\bar{\omega}\tau}, \qquad v = C_2 h \cos(\xi)\sin(\eta)\, e^{i\bar{\omega}\tau},$$

$$w = C_3 h \sin(\xi)\sin(\eta)\, e^{i\bar{\omega}\tau}, \qquad \Psi_x = C_4 \cos(\xi)\sin(\eta)\, e^{i\bar{\omega}\tau},$$

$$\Psi_y = C_5 \sin(\xi)\cos(\eta)\, e^{i\bar{\omega}\tau}, \tag{28}$$

where $\xi = m\pi x/a$ and $\eta = n\pi y/b$. $C_i, \bar{\omega}$, and τ are coefficients, frequency and time, respectively.

The plate characteristic equation can be found by substituting equation (28) into the equation of motion (24). A set of five homogeneous equations can be obtained as

$$K_{ij} C_j = 0 \qquad i, j = 1, \ldots, 5 \tag{29}$$

where k_{ij} are listed in the Appendix, equation (A4). For non-zero solutions to exist, the determinant of the coefficient matrix [K] must vanish, enabling evaluation of the eigenvalues for plate stability and vibration under initial stresses.

5. RESULTS AND DISCUSSIONS

The material properties of a carbon/epoxy system have been used in the numerical examples. The constants used are $E_{33} = 180$ GPa, $E_{11} = 20$ GPa, $G_{13} = 12$ GPa, $v_{31} = 0{\cdot}4$, $v_{12} = 0{\cdot}3$ for the fiber, and $E_m = 5{\cdot}0$ GPa, $v_m = 0{\cdot}3$ for the matrix. The fiber volume fraction is assumed to be 0·65. Using these constants, the reduced stiffnesses for fiber and matrix, as required by equation (5), can be calculated. The fiber is transversely isotropic although all the theoretical formulations are not restricted to this.

The most fundamental issue concerning such a composite is probably the resulting elastic stiffness. Figure 5 shows the relation between fiber orientation and Young's moduli E_x, E_y, and E_z. When both θ_0 and ϕ_0 are small, most fibers are closely aligned with the x-axis, resulting in a rather high E_x and low E_y and E_z. When θ_0 increases, E_x drops rapidly until about $\theta_0 = 135°$, where a minimum is reached. E_y reaches a maximum at about

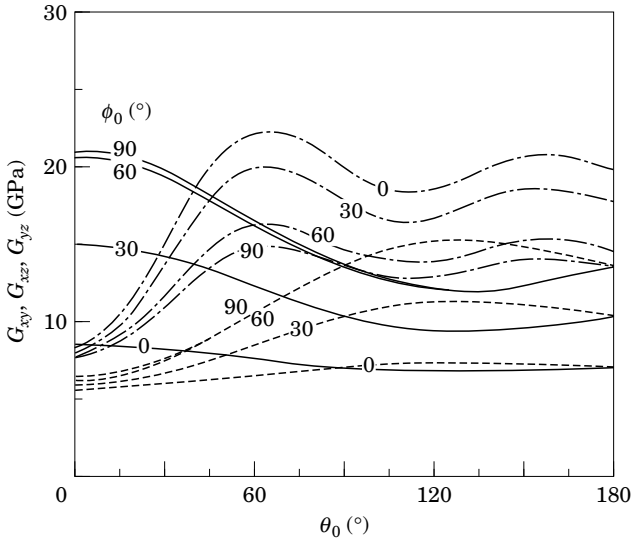

Figure 6. Shear moduli versus θ_0 for various ϕ_0: —·—, G_{xy}; ——, G_{xz}; – – –, G_{yz}.

$\theta_0 = 120^\circ$. The transverse modulus E_z is independent of θ_0. The composite is isotropic and these moduli are identical when $\theta_0 = 180^\circ$ and $\phi_0 = 90^\circ$. Results for shear moduli are shown in Figure 6. G_{xy} is significantly increased with θ_0 when $\theta_0 \leqslant 60^\circ$, followed by a wave-like variation. On the other hand, G_{xz} drops slowly when θ_0 is increased up to about $\theta_0 = 130^\circ$. As ϕ_0 increases, it is found that all the transverse moduli (E_z, G_{xz}, G_{yz}) increase, while all the in-plane moduli (E_x, E_y, G_{xy}) decrease.

Typical results for the plate fundamental frequencies under the initial stresses σ_{x0} and σ_{y0} are shown in Figure 7. It is found that the fundamental frequencies are increased when either σ_{x0} or σ_{y0} is increased; this is simply due to plate tensioning. When both σ_{x0} and σ_{y0}

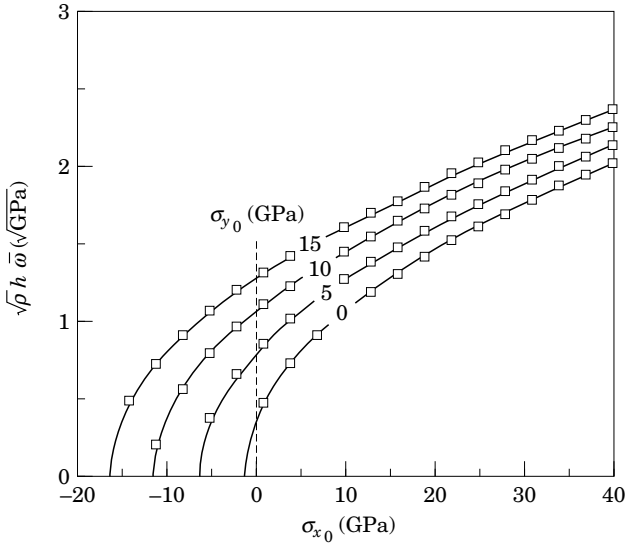

Figure 7. Fundamental frequencies of the plate under initial σ_{x_0} and σ_{y_0} (GPa): ($a/t = 10$, $b/t = 10$, $\theta_0 = 0{\cdot}1$, and $\phi_0 = 0{\cdot}2$).

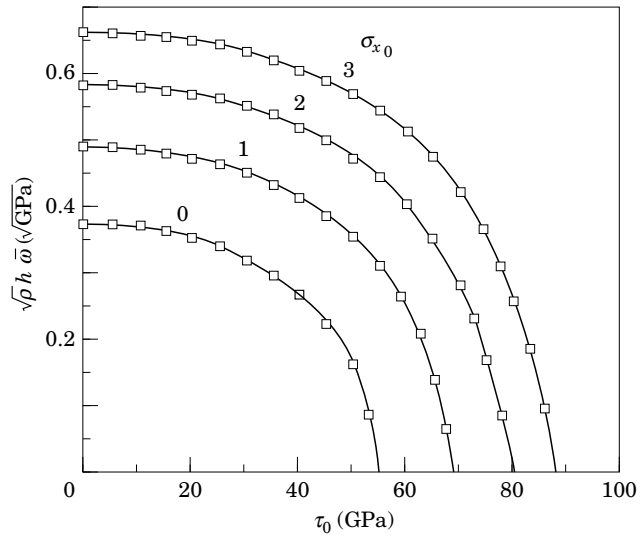

Figure 8. Fundamental frequencies of the plate under τ_0 and σ_{x_0} (GPa): ($a/t = 10$, $b/t = 10$, $\theta_0 = 0{\cdot}1$, and $\phi_0 = 0{\cdot}2$).

vanish, the point corresponds to the natural frequency. As σ_{x0} becomes negative, the fundamental frequency will eventually vanish as the compressive stress increases, resulting in plate buckling. Higher compressive stress is required to buckle the plate if the tensile stress in other directions (σ_{y0}) increases. Figure 8 illustrates the effect of initial shear stresses on the fundamental frequency of the plate. As τ_0 increases, the fundamental frequencies are reduced and will eventually vanish when plate buckling due to the initial shear stress occurs. Unlike the normal stresses, positive and negative shear stresses yield the same results for fundamental frequencies and buckling loads. It should be noted that the results in Figures 7 and 8 are the lowest, and the corresponding mode is $m = n = 1$; it is possible

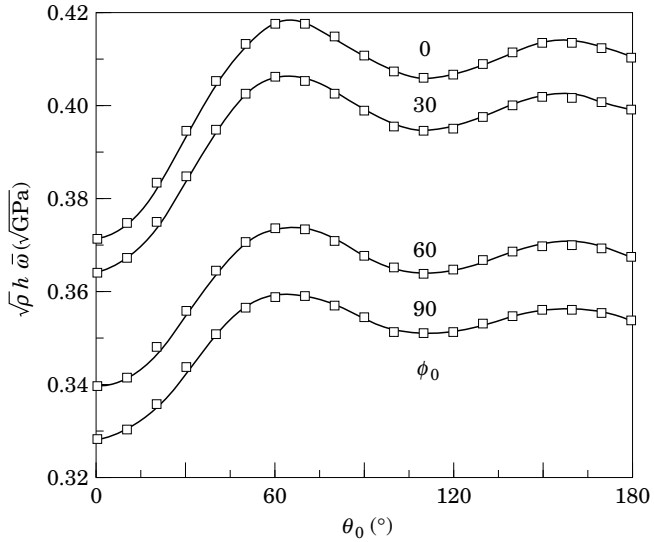

Figure 9. Influence of θ_0 on the natural frequencies ($a/t = 10$, $b/t = 10$) with varying ϕ_0 (°).

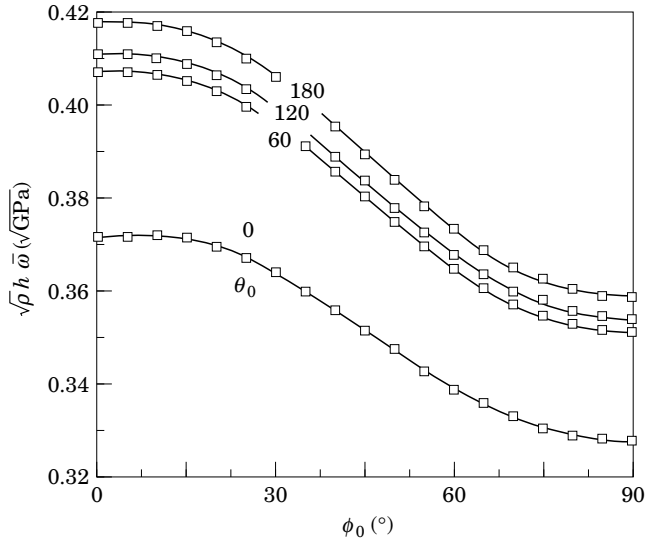

Figure 10. Influence of ϕ_0 on the natural frequencies ($a/t = 10$, $b/t = 10$) with varying θ_0 (°).

that the lowest results can occur in other mode shapes if the plate aspect ratio, material constants, or fiber orientation are changed.

The effect of fiber orientation on the natural frequency of the plate is shown in Figures 9 and 10. As the plate natural frequency is dependent on the plate rigidity, it is expected that the Young's and shear moduli are crucial to the problem. Among six elastic moduli, the in-plane ones (E_x, E_y, G_{xy}) are dominant terms, whereas the transverse moduli (E_z, G_{xz}, G_{yz}) will not influence the plate vibration and buckling unless the plate is thick enough. As θ_0 is increased, the frequencies follow wave-like curves due to opposite trends

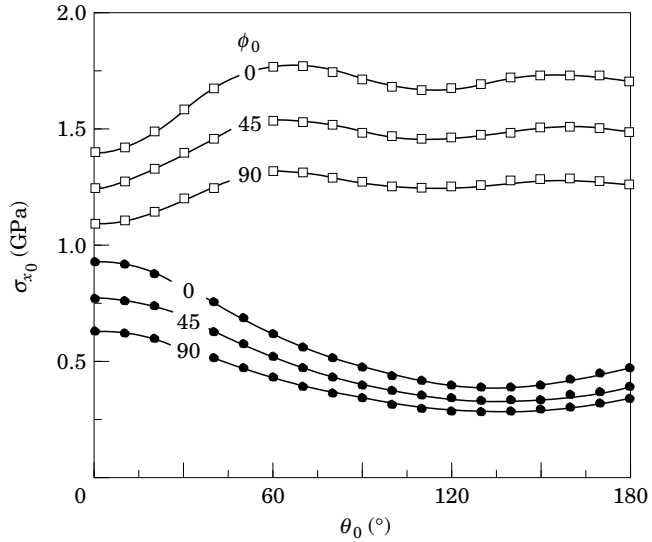

Figure 11. Critical initial stress σ_{x_0} for plate buckling ($a/t = 10$) for varying, ϕ_0 (°). b/t: —□—, 10; —●—, 100.

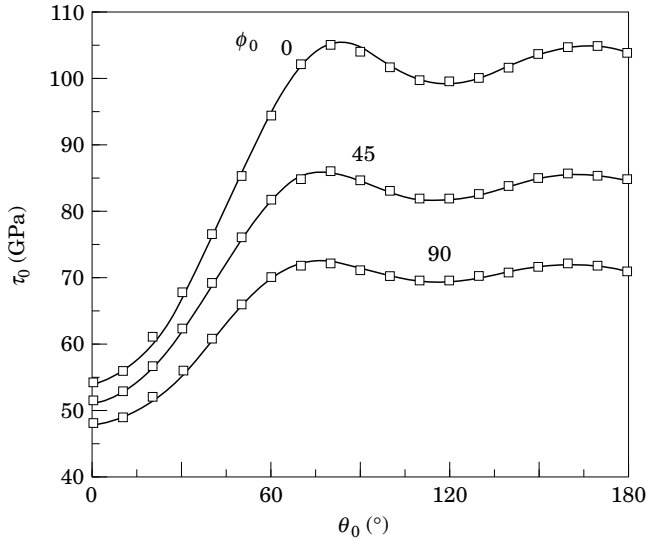

Figure 12. Critical initial shear stress τ_0 for plate buckling ($a/t = 10$, $b/t = 10$) with varying ϕ_0 (°).

by E_x and E_y. On the other hand, when ϕ_0 increases, all three in-plane moduli are found to be reduced, and, as a result, the frequencies are monotonously decreased.

The plate buckling behavior is generally controlled by three factors: stiffness, structure geometry, and loading type. Unlike beam buckling, which is dominated solely by the longitudinal modulus, all in-plane moduli can be crucial to plate buckling. This fact is illustrated in Figure 11 showing the critical normal stress σ_{x_0} for plate buckling as a function of plate aspect ratio and θ_0. For a square plate ($a/t = 10$, $b/t = 10$), the σ_{x_0} is increased as θ_0 increased until about $\theta_0 = 60^\circ$, followed by a slightly wavy variation. On the other hand, when the plate is long in the y-direction ($a/t = 10$, $b/t = 100$), the influence of E_y and G_{xy} becomes minimal. In this case, the plate buckling behaves like a beam buckling and the critical load curves are found to be very similar to the E_x curves in Figure 5. Figure 12 shows the roles of θ_0 and ϕ_0 in the critical initial shear stress for a square plate. The results are quite similar to the G_{xy} in Figure 12, suggesting that the in-plane shear modulus is the dominant term for this problem.

It should be noted that the results in Figures 7–12, based upon $m = n = 1$, are the lowest compared with other modes. However, for a long plate subjected to initial shear stresses such as the case studied ($a/t = 10$, $b/t = 100$), the lowest critical loads are found to occur at rather high vaules of n. Shown in Figure 13 are the critical shear stresses for different modes. It is found that the lowest values depend not only on the mode but also on the θ_0 and ϕ_0. For the case examined, the corresponding mode having lowest shear stress is $m = 1$ and $n = 16$ at θ_0 up to about 60°, beyond which the corresponding mode varies among $n = 8$–13.

6. CONCLUSIONS

Introduced in this paper are three orthotropic constants, which enable the stiffness transformation to be greatly simplified. Based upon the aggregated model, the elastic constants of a composite composed of spatially distributed fibers have been explicitly evaluated. The fiber orientation is described by a two-parameter function to simulate a bias distribution. The six composite moduli have been found to vary monotonously with

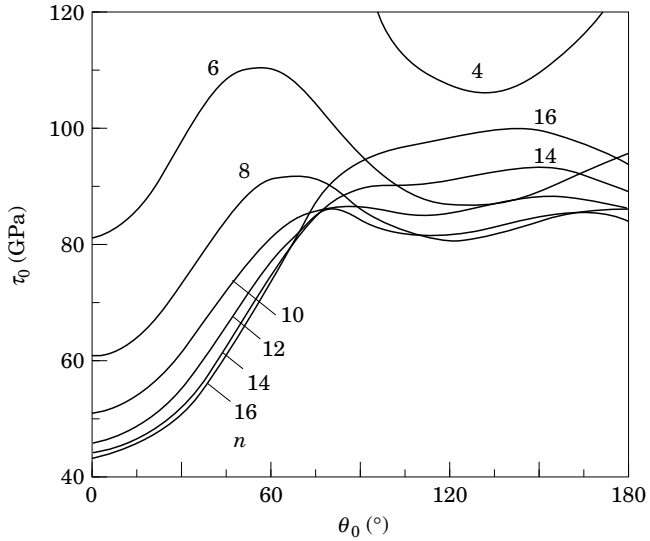

Figure 13. Influence of ϕ_0 and buckling mode on critical τ_0 ($a/t = 10$, $b/t = 100$, $\phi_0 = 45^\circ$, $m = 1$), for various modes (n).

ϕ_0, while they follow wave-like curves with θ_0 except E_2. Using the virtual work theorem and Trefftz stress components, the equations of equilibrium of the composite plate under initial stresses have been obtained and applied to evaluate the fundamental frequencies of the plate. The role of ϕ_0 on plate behavior is quite predictable; an increase in ϕ_0 results in lower in-plane moduli, which in turn lead to lower vibration frequencies and buckling loads. For θ_0, however, its influence is affected by other factors such as the type of initial stress, mode shape and aspect ratio. Numerical examination is therefore necessary to determine the effect of θ_0 on the plate behavior.

ACKNOWLEDGMENTS

The authors wish to thank the National Science Council of Taiwan, R.O.C. for the support of this research (NSC 85-2216-E-035-012).

REFERENCES

1. P. J. Hine, R. A. Duckett, N. Davidson and A. R. Clarke 1993 *Composite Science and Technology* **47**, 65–73. Modelling the elastic properties of fiber-reinforced composites: I—Orientation measurement.
2. S. W. Yurgartis and K. Morey 1993 *Composite Science and Technology* **46**, 39–50. Measurement of yarn shape and nesting in plain-weave composites.
3. F. Gadala-Maria and F. Parsi 1993 *Polymer Composites* **14**, 126–131. Measurement of fiber orientation in short-fiber composites using digital image processing.
4. T. Mura 1987 *Micromechanics of Defects in Solids*. Dordrecht: Martinus Nijhoff Publishers, second edition.
5. J. D. Eshelby 1957 *Proceedings of the Royal Society of London* **A241**, 376–396. The determination of the elastic field of an ellipsoidal inclusion and related problems.
6. T. Mori and K. Tanaka 1973 *Acta Metallica* **21**, 571–574. Average stress in matrix and average energy of materials with misfitting inclusions.
7. R. M. Christensen and F. M. Waals 1972 *Journal of Composite Materials*, **6**, 518–532. Effective stiffness of randomly oriented fiber composites.

8. J. C. Halpin, K. Jerine and J. M. Whitney 1971 *Journal of Composite Materials* **5**, 36–49. The laminate analogy for two- and three-dimensional composite materials.
9. I. H. Yang and W. S. Kuo 1993 *Journal of Sound and Vibration* **168**, 285–297. Stability and vibration of initially stresses thick laminated plates.
10. I. H. Yang and W. S. Kuo 1992 *The Aeronautical Journal of the Royal Aeronautical Society* **96**, 313–318. Generic buckling of thick orthotropic cylindrical shells.
11. W. S. Kuo and I. H. Yang 1989 *International Journal of Mechanical Science* **31**, 131–143. Generic non-linear behavior of antisymmetric angle-ply laminated plates.
12. V. V. Novozhilov 1953 *Foundations of the Non-linear Theory of Elasticity*. Rochester, New York: Graylock Press.
13. V. V. Bolotin 1963 *Non-conservative Problems of the Theory of Elastic Stability*. New York: MacMillan.
14. C. T. Sun and S. Li 1988 *Journal of Composite Materials* **22**, 629–639. Three-dimensional effective elastic constants for thick laminates.
15. Z. Hashin and W. Rosen 1964 *Journal of Applied Mechanics* **31**, 223–232. The elastic moduli of fiber reinforced materials.
16. R. M. Christensen and F. M. Waals 1972 *Journal of Composite Materials* **6**, 518–532. Effective stiffness of randomly oriented fiber composites.
17. C. C. Chao, T. P. Tung, C. C. Sheu and J. H. Tseng 1994 *Journal of Vibration and Acoustics* **116**, 371–378. A consistent higher-order theory of laminated plates with non-linear impact model analysis.
18. C. C. Chao, T. P. Tung and H. H. Li 1994 *Journal of Energy Resources Technology* **116**, 240–249. 3-D stress analysis of cross-ply laminated composites.

APPENDIX

ELEMENTS IN THE STRESS TRANSFORMATION [T]

$$T_{11} = (mpr - ns)^2, \qquad T_{12} = (ms + npr)^2, \qquad T_{13} = q^2r^2,$$

$$T_{14} = -2npqr^2 - 2mqrs, \qquad T_{15} = -2mpqr^2 + 2nqrs, \qquad T_{16} = 2(npr + ms)(mpr - ns),$$

$$T_{21} = (mps + nr)^2, \qquad T_{22} = (mr + nps)^2, \qquad T_{23} = q^2s^2,$$

$$T_{24} = 2mqrs - 2npqs^2, \qquad T_{25} = -2nqrs - 2mpqs^2, \qquad T_{26} = 2(nr + mps)(-mr + nps),$$

$$T_{31} = m^2q^2, \qquad T_{32} = n^2q^2, \qquad T_{33} = p^2,$$

$$T_{34} = 2npq, \qquad T_{35} = 2mpq, \qquad T_{36} = 2mnq^2, \qquad T_{41} = -mnqr - m^2pqs,$$

$$T_{42} = mnqr - n^2pqs, \qquad T_{43} = pqs, \qquad T_{44} = mpr - np^2s + nq^2s,$$

$$T_{45} = -npr - mp^2s + mq^2s, \qquad T_{46} = m^2qr - n^2qr - 2mnpqs,$$

$$T_{51} = m^2pqr - mnqs, \qquad T_{52} = n^2pqr + mnqs, \qquad T_{53} = -pqr,$$

$$T_{54} = np^2r - nq^2r + mps, \qquad T_{55} = mp^2r - mq^2r - nps, \qquad T_{56} = 2mnpqr + m^2qs - n^2qs,$$

$$T_{61} = (-mpr + ns)(nr + mps), \qquad T_{62} = (npr + ms)(mr - nps), \qquad T_{63} = -q^2rs,$$

$$T_{64} = -mqr^2 + 2npqrs + mqs^2, \qquad T_{65} = nqr^2 + 2mpqrs - nqs^2,$$

$$T_{66} = p(r^2 - s^2)(m^2 - n^2) - 2mnrs(1 + p^2). \tag{A1}$$

TRANSFORMATION FOR $\bar{Q}_{ij}$

$$\begin{aligned}\bar{Q}_{11} &= Q_{11}(mpr - ns)^2 + Q_{22}(mps + nr)^2 + Q_{33}m^2q^2 - K_1m^2q^2(mps + nr)^2 \\ &\quad - K_2m^2q^2(mpr - ns)^2 - K_3(mpr - ns)^2(mps + nr)^2, \\ \bar{Q}_{12} &= Q_{12}p^2 + Q_{13}q^2s^2 + Q_{23}q^2r^2 + K_1mnq^2(mps + nr)(mr - nps) \\ &\quad + K_2mnq^2(ns - mpr)(ms + npr) \\ &\quad + K_3(mpr - ns)(ms + npr)(mps + nr)(mr - nps).\end{aligned}$$

$$\bar{Q}_{13} = Q_{12}n^2q^2 + Q_{13}(mr - nps)^2 + Q_{23}(ms + npr)^2 + K_1mpq^2s(mps + nr)$$
$$+ K_2mpq^2r(mpr - ns) + K_3q^2rs(ns - mpr)(mps + nr),$$

$$\bar{Q}_{14} = \frac{q}{2}[-2Q_{12}np + 2Q_{13}s(nps - mr) + 2Q_{23}r(ms + npr)$$
$$+ K_1m(mps + nr)(nq^2s - np^2s + mpr)$$
$$+ K_2m(mpr - ns)(nq^2r - np^2r - mps)$$
$$+ K_3(mpr - ns)(mps + nr)(2nprs - mr^2 + ms^2)],$$

$$\bar{Q}_{15} = \frac{q}{2}[-Q_{11}r(mpr - ns) - Q_{22}s(mps + nr) + Q_{33}mp$$
$$+ K_1m(mps + nr)(mq^2s - mp^2s - npr)$$
$$+ K_2m(mpr - ns)(mq^2r - mp^2r + nps)$$
$$+ K_3(mpr - ns)(mps + nr)(2mprs + nr^2 - ns^2)],$$

$$\bar{Q}_{16} = \tfrac{1}{2}\{Q_{11}(mpr - ns)(ms + npr) + Q_{22}(mps + nr)(nps - mr) + Q_{33}mnq^2$$
$$- K_1mq^2(mps + nr)(2mnps - m^2r + n^2r)$$
$$- K_2mq^2(mpr - ns)(2mnpr + m^2s - n^2s)$$
$$- K_3(mpr - ns)(mps + nr)[2mnrs(p^2 + 1) - p(m^2 - n^2)(r^2 - s^2)]\}$$

$$\bar{Q}_{22} = Q_{11}(ms + npr)^2 + Q_{22}(nps - mr)^2 + Q_{33}n^2q^2 - K_1n^2q^2(mr - nps)^2$$
$$- K_2n^2q^2(ms + npr)^2 - K_3(ms + npr)^2(mr - nps)^2$$

$$\bar{Q}_{23} = Q_{12}m^2q^2 + Q_{13}(mps + nr)^2 + Q_{23}(mpr - ns)^2 + K_1npq^2s(nps - mr)$$
$$+ K_2npq^2r(ms + npr) + K_3q^2rs(ms + npr)(mr - nps),$$

$$\bar{Q}_{24} = \frac{q}{2}[-Q_{11}r(ms + npr) - Q_{22}s(nps - mr) + Q_{33}np$$
$$+ K_1n(nps - mr)(nq^2s - np^2s + mpr)$$
$$+ K_2n(ms + npr)(nq^2r - np^2r - mps)$$
$$+ K_3(ms + npr)(nps - mr)(2nprs - mr^2 + ms^2)],$$

$$\bar{Q}_{25} = \frac{q}{2}[-2Q_{12}mp + 2Q_{13}s(mps + nr) + 2Q_{23}r(mps - ns)$$
$$+ K_1n(nps - mr)(mq^2s - mp^2s - npr)$$
$$+ K_2n(ms + npr)(mq^2r - mp^2r + nps)$$
$$+ K_3(ms + npr)(nps - mr)(2mprs + nr^2 - ns^2)],$$

$$\bar{Q}_{26} = \tfrac{1}{2}\{Q_{11}(mpr - ns)(ms + npr) + Q_{22}(mps + nr)(nps - mr) + Q_{33}mnq^2$$
$$- K_1nq^2(nps - mr)(2mnps - m^2r + n^2r)$$
$$- K_2nq^2(ms + npr)(2mnpr + m^2s - n^2s)$$
$$- K_3(ms + npr)(nps - mr)[2mnrs(p^2 + 1) - p(m^2 - n^2)(r^2 - s^2)]\},$$

$$\bar{Q}_{33} = Q_{11}q^2r^2 + Q_{22}q^2s^2 + Q_{33}p^2 - K_1p^2q^2s^2 - K_2p^2q^2r^2 - K_3q^4r^2s^2,$$

$$\begin{aligned}
\bar{Q}_{34} &= \frac{q}{2}[-Q_{11}r(ms+npr) - Q_{22}s(nps-mr) + Q_{33}np \\
&\quad + K_1ps(np^2s - nq^2s - mpr) + K_2pr(np^2r - nq^2r + mps) \\
&\quad + K_3q^2rs(2nprs - mr^2 + ms^2)],
\end{aligned}$$

$$\begin{aligned}
\bar{Q}_{35} &= \frac{q}{2}[-Q_{11}r(mpr-ns) - Q_{22}s(mps+nr) + Q_{33}mp + K_1ps(mp^2s - mq^2s + npr) \\
&\quad + K_2pr(mp^2r - mq^2r - nps) + K_3q^2rs(2mprs + nr^2 - ns^2)], \\
\bar{Q}_{36} &= -Q_{12}mnq^2 + Q_{13}(mps+nr)(mr-nps) + Q_{23}(ns-mpr)(ms+npr) \\
&\quad + K_1pq^2s[mnps - (r/2)(m^2-n^2)] + K_2pq^2r[mnpr + (s/2)(m^2-n^2)] \\
&\quad - K_3q^2rs[mnrs(p^2+1) - (p/2)(m^2-n^2)(r^2-s^2)], \\
\bar{Q}_{44} &= Q_{44}(mpr-ns)^2 + Q_{55}(mps+nr)^2 + Q_{66}m^2q^2 + K_1npq^2s(nps-mr) \\
&\quad + K_2npq^2r(ms+npr) + K_3q^2rs(ms+npr)(mr-nps), \\
\bar{Q}_{45} &= -Q_{44}(mpr-ns)(ms+npr) - Q_{55}(mps+nr)(nps-mr) - Q_{66}mnq^2 \\
&\quad + K_1pq^2s[mnps - (r/2)(m^2-n^2)] + K_2pq^2r[mnpr + (s/2)(m^2-n^2)] \\
&\quad - K_3q^2rs[mnrs(p^2+1) - (p/2)(m^2-n^2)(r^2-s^2)],
\end{aligned}$$

$$\begin{aligned}
\bar{Q}_{46} &= \frac{q}{2}[2Q_{44}r(mpr-ns) + 2Q_{55}s(mps+nr) - 2Q_{66}mp \\
&\quad + K_1n(nps-mr)(mq^2s - mp^2s - npr) \\
&\quad + K_2n(ms+npr)(mq^2r - mp^2r + nps) \\
&\quad + K_3(ms+npr)(2mprs + nr^2 - ns^2)(nps-mr)], \\
\bar{Q}_{55} &= Q_{44}(ms+npr)^2 + Q_{55}(nps-mr)^2 + Q_{66}n^2q^2 + K_1mpq^2s(mps+nr) \\
&\quad + K_2mpq^2r(mpr-ns) - K_3q^2rs(mpr-ns)(mps+nr),
\end{aligned}$$

$$\begin{aligned}
\bar{Q}_{56} &= \frac{q}{2}[2Q_{44}r(ms+npr) + 2Q_{55}s(nps-mr) - 2Q_{66}np \\
&\quad + K_1m(mps+nr)(nq^2s - np^2s + mpr) \\
&\quad + K_2m(mpr-ns)(nq^2r - np^2r - mps) \\
&\quad + K_3(mpr-ns)(mps+nr)(2nprs - mr^2 + ms^2)], \\
\bar{Q}_{66} &= Q_{44}q^2r^2 + Q_{55}q^2s^2 + Q_{66}p^2 + K_1mnq^2(mps+nr)(mr-nps) \\
&\quad + K_2mnq^2(ns-mpr)(ms+npr) \\
&\quad + K_3(mpr-ns)(ms+npr)(mps+nr)(mr-nps).
\end{aligned} \tag{A2}$$

COEFFICIENTS IN EQUATION (24)

$$\begin{aligned}
H_1 &= A_{11}u_{,xx} + A_{66}u_{,yy} + (A_{12}+A_{66})v_{,xy} - \rho h\ddot{u} + \bar{N}_x u_{,xx} + \bar{N}_y u_{,yy} + 2\bar{M}_{xy}\Psi_{x,xy}, \\
H_2 &= A_{22}v_{,yy} + A_{66}v_{,xx} + (A_{12}+A_{66})u_{,xy} - \rho h\ddot{v} + \bar{N}_x v_{,xx} + \bar{N}_y v_{,yy} + 2\bar{M}_{xy}\Psi_{y,xy}, \\
H_3 &= A_{55}w_{,xx} + A_{44}w_{,yy} + A_{55}\Psi_{x,x} + A_{44}\Psi_{y,y} - \rho h\ddot{w} + \bar{N}_x w_{,xx} + \bar{N}_y w_{,yy}, \\
H_4 &= -A_{55}w_{,x} - A_{55}\Psi_x + D_{11}\Psi_{x,xx} + D_{66}\Psi_{x,yy} + (D_{12}+D_{66})\Psi_{y,xy} - \tfrac{1}{12}\rho h^3\ddot{\Psi}_x \\
&\quad + 2\bar{M}_{xy}u_{,xy} + \bar{M}_x^*\Psi_{x,xx} + \bar{M}_y^*\Psi_{x,yy},
\end{aligned}$$

$$H_5 = -A_{44}w_{,y} - A_{44}\Psi_y + D_{22}\Psi_{y,yy} + D_{66}\Psi_{y,xx} + (D_{12} + D_{66})\Psi_{x,xy} - \tfrac{1}{12}\rho h^3\ddot{\Psi}_y + 2\bar{M}_{xy}v_{,xy} + \bar{M}_x^*\Psi_{y,xx} + \bar{M}_y^*\Psi_{y,yy},$$

$$I_1 = A_{66}u_{,y} + A_{66}v_{,x} + \bar{M}_{xy}\Psi_{x,x}, \qquad I_2 = A_{12}u_{,x} + A_{22}v_{,x} + \bar{M}_{xy}\Psi_{y,x},$$

$$I_3 = A_{44}w_{,y} + A_{44}\Psi_y + \bar{N}_y w_{,y}, \qquad I_4 = D_{66}\Psi_{x,y} + D_{66}\Psi_{y,x} + \bar{M}_y^*\Psi_{x,y},$$

$$I_5 = D_{12}\Psi_{x,x} + D_{22}\Psi_{y,y} + \bar{M}_y^*\Psi_{y,y}, \qquad J_1 = A_{11}u_{,x} + A_{12}v_{,y} + \bar{M}_{xy}\Psi_{x,y},$$

$$J_2 = A_{66}v_{,x} + A_{66}u_{,y} + \bar{M}_{xy}\Psi_{y,y}, \qquad J_3 = A_{55}w_{,x} + A_{55}\Psi_x + \bar{N}_x w_{,x},$$

$$J_4 = D_{11}\Psi_{x,x} + D_{12}\Psi_{y,x} + \bar{M}_x^*\Psi_{x,x}, \qquad J_5 = D_{66}\Psi_{x,y} + D_{66}\Psi_{y,x} + \bar{M}_x^*\Psi_{y,x}. \tag{A3}$$

COEFFICIENTS IN K_{ij}

$$K_{11} = \hat{Q}_{11}\lambda_x^2 + \hat{Q}_{66}\lambda_y^2 - \rho h^2\bar{\omega}^2 + \sigma_{x_0}\lambda_x^2 + \sigma_{y_0}\lambda_y^2, \qquad K_{12} = (\hat{Q}_{12} + \hat{Q}_{66})\lambda_x\lambda_y,$$

$$K_{14} = \tfrac{1}{3}\tau_0\lambda_x\lambda_y, \qquad K_{22} = \hat{Q}_{22}\lambda_y^2 + \hat{Q}_{66}\lambda_x^2 - \rho h^2\bar{\omega}^2 + \sigma_{x_0}\lambda_x^2 + \sigma_{y_0}\lambda_y^2, \qquad K_{25} = \tfrac{1}{3}\tau_0\lambda_x\lambda_y,$$

$$K_{33} = \hat{Q}_{55}\lambda_x^2 + \hat{Q}_{44}\lambda_y^2 - \rho h^2\bar{\omega}^2 + \sigma_{x_0}\lambda_x^2 + \sigma_{y_0}\lambda_y^2, \qquad K_{34} = \hat{Q}_{55} + \lambda_x, \qquad K_{35} = \hat{Q}_{44}\lambda_y,$$

$$K_{44} = \hat{Q}_{55} + \tfrac{1}{12}\hat{Q}_{11}\lambda_x^2 + \tfrac{1}{12}\hat{Q}_{66}\lambda_y^2 - \tfrac{1}{12}\rho h^2\bar{\omega}^2 + \tfrac{1}{12}\sigma_{x_0}\lambda_x^2 + \tfrac{1}{12}\sigma_{y_0}\lambda_y^2,$$

$$K_{45} = \tfrac{1}{12}(\hat{Q}_{12} + \hat{Q}_{66})\lambda_x\lambda_y,$$

$$K_{55} = \hat{Q}_{44} + \tfrac{1}{12}\hat{Q}_{22}\lambda_y^2 + \tfrac{1}{12}\hat{Q}_{66}\lambda_x^2 - \tfrac{1}{12}\rho h^2\bar{\omega}^2 + \tfrac{1}{12}\sigma_{x_0}\lambda_x^2 + \tfrac{1}{12}\sigma_{y_0}\lambda_y^2, \tag{A4}$$

where

$$\lambda_x = m\pi h/a \text{ and } \lambda_y = n\pi h/b.$$